



Research Note

Optimal tracking control of an underactuated container ship based on direct Gauss pseudospectral method

M.T. Ghorbani and H. Salarieh*

School of Mechanical Engineering, Sharif University of Technology, Tehran, P.O. Box 111559567, Iran.

Received 10 September 2012; received in revised form 18 January 2014; accepted 9 March 2014

KEYWORDS

Optimal control;
Tracking;
Ship control;
Gauss pseudospectral
transcription;
Nonlinear
programming.

Abstract. In this paper, the problem of optimal tracking control for a container ship is addressed. The multi-input-multi-output nonlinear model of the S175 container ship is well established in the literature and represents a challenging problem for control design, where the design requirement is to follow a commanded maneuver at a desired speed. To satisfy the constraints on the states and control inputs of the vessel nonlinear dynamics and minimize the heading error, a nonlinear optimal controller is formed. To solve the resulted nonlinear constrained optimal control problem, the Gauss Pseudospectral Method (GPM) is used to transcribe the optimal control problem into a Nonlinear Programming Problem (NLP) by discretization of states and controls. The resulted NLP is then solved by a well-developed algorithm known as SNOPT. The results for course-keeping and course-changing autopilots illustrate the effectiveness of the proposed approach in dealing with vessel tracking control.

© 2014 Sharif University of Technology. All rights reserved.

1. Introduction

The problem of the tracking control of marine vehicles is a highly important issue, especially for autopilot design. There are some challenges in this area. The first is that the vessels are often underactuated. Advanced techniques in the field of control of underactuated systems [1-3] have been suggested for path planning of a 3-DoF vessel (surge, sway and yaw motion) with two independent inputs.

Another difficulty for the tracking control of marine surface vessels is the intrinsic physical limitations in the control inputs. The rudder deflection angle and its rate have operating limits which should be considered. In addition, the controller must

consider safety constraints. Since the roll motion of the marine vehicle is the principal cause for the probabilities of slamming and deck wetness [4], enforcing roll constraints while maneuvering in seaways becomes an important designation in surface vessel control.

To overcome the mentioned challenges, some control design methods have been developed. Li et al. (2009) used Model Predictive Control (MPC) to control both the cross tracking and heading error by the rudder angle for an underactuated surface vessel while considering rudder limitation and roll constraints [5]. MPC can handle underactuated problems by combining all the objectives into a single objective function. However, due to computational complexity, the MPC applications for systems with fast dynamics are not very common [6]. In addition, Li et al. (2009) used a reduced order linear model for MPC implementation. In general, the linear models result in the loss of vital mathematical information from the dynamics of the

*. Corresponding author. Tel.: +98 21 66165538;
Fax: +98 21 66000021
E-mail addresses: mt_ghorbani@alum.sharif.edu (M.T. Ghorbani); salarieh@sharif.edu (H. Salarieh)

physical systems, and their valid range of operation is small. A better choice to tackle tracking control problems, while satisfying the input and state constraints, is nonlinear optimal control. Nonlinear optimal control satisfies any of the desirable constraints, and is also suitable for nonlinear systems [7]. In an optimal control problem, the goal is determination of the states and controls that minimize a cost functional subject to nonlinear dynamic constraints, boundary conditions and inequality path constraints. There are two methods for resolving optimal control problems: direct and indirect [8]. In an indirect method, first-order necessary conditions for optimality are derived from the optimal control problem via the calculus of variations and Pontryagin's minimum principle [9]. These necessary conditions form a Hamiltonian Boundary-Value Problem (HBVP), which is then solved numerically for extremal trajectories. The optimal solution is then found by choosing the extremal trajectory with the lowest cost. The primary advantages of indirect methods are high accuracy in the solution and the assurance that the solution satisfies the first-order optimality conditions. However, indirect methods have several disadvantages. First, the solution of HBVP must be usually derived analytically, which can be often non-trivial. Second, if one wishes to obtain the solution numerically, as numerical techniques used in indirect methods typically have small radii of convergence, an extremely good initial guess of the unknown solution or boundary conditions is generally required. Finally, for problems with path constraints, it is necessary to have a priori knowledge about the constrained and unconstrained arcs or switching structure [10]. Çimen and Banks (2004) used the indirect method to solve nonlinear optimal tracking control of an oil tanker [7].

On the other hand, the direct methods transform the optimal control problem into a nonlinear programming problem (NLP). Direct methods have the advantage that the first-order necessary conditions do not need to be derived. Furthermore, they have much larger radii of convergence than indirect methods and, thus, do not require as good an initial guess. Lastly, the switching structure does not need to be known a priori [10]. In this paper, to solve a nonlinear 4-DoF tracking control problem for an underactuated container ship, we address a kind of direct method, known as the Gauss Pseudospectral Method (GPM), to transform the optimal control problem into an NLP by parameterization of the states and the controls. These parameterization techniques have an important role to play in the convergence and accuracy of the solution, and low computation time [11]. The resulted NLP is then solved by a well-developed algorithm called SNOPT. The proposed method is suitable for autopilot design and provides

tracking of a commanded course heading at a desired shaft velocity, while satisfying the roll and rudder constraints.

This paper is organized as follows: First, the Gauss pseudospectral method is presented in its most current form, and a complete NLP is provided which includes both path constraints and differential equations in the optimal control problem formulation. Afterwards, the vessel dynamical model adopted in the controller design is presented. Section 4 presents the simulation results, together with some discussions, and the last section provides some concluding remarks.

2. Gauss pseudospectral method

Consider the following general optimal control problem. The objective is to determine the state, $\mathbf{x}(t)$, and control, $\mathbf{u}(t)$, that minimize the given cost functional:

Minimize:

$$J = \Phi(\mathbf{x}(t_0), t_0, \mathbf{x}(t_f), t_f) + \int_{t_0}^{t_f} g(\mathbf{x}(t), \mathbf{u}(t), t) dt.$$

s.t.:

$$\left\{ \begin{array}{l} \text{The dynamic constraints:} \\ \quad \dot{\mathbf{x}}(t) = \mathbf{f}(\mathbf{x}(t), \mathbf{u}(t), t), t \in [t_0, t_f] \\ \text{The boundary conditions:} \\ \quad \mathbf{h}(\mathbf{x}(t_0), t_0, \mathbf{x}(t_f), t_f) = \mathbf{0} \\ \text{The inequality path constraints:} \\ \quad \mathbf{C}(\mathbf{x}(t), \mathbf{u}(t), t) \leq \mathbf{0}, \end{array} \right. \quad (1)$$

where t_0 is the fixed or free initial time, t_f is the fixed or free final time, and $t \in [t_0, t_f]$. The terms, Φ and g , are called the endpoint cost and Lagrangian, respectively. The functions, \mathbf{f} , \mathbf{h} and \mathbf{C} , are known and smooth functions which denote the dynamical system, boundary conditions, and inequality constraints on the path, respectively. Eq. (1) is referred to as the continuous Bolza problem [10]. The GPM method requires a fixed time interval, such as $[-1, 1]$. So, the time variable is mapped to the general interval, $\tau \in [-1, 1]$, via the affine transformation:

$$\tau = \frac{2t}{t_f - t_0} - \frac{t_f + t_0}{t_f - t_0}.$$

Now, the optimal control problem is rewritten as:

$$J = \Phi(\mathbf{x}(\tau_0), \tau_0, \mathbf{x}(\tau_f), \tau_f) + \frac{t_f - t_0}{2} \int_{\tau_0}^{\tau_f} g(\mathbf{x}(\tau), \mathbf{u}(\tau); t_0, t_f) d\tau,$$

s.t.:

$$\left\{ \begin{array}{l} \text{The dynamic constraints:} \\ \frac{d\mathbf{x}}{d\tau} = \frac{t_f - t_0}{2} \mathbf{f}(\mathbf{x}(\tau), \mathbf{u}(\tau), \tau; t_0, t_f) \\ \text{The boundary conditions:} \\ \mathbf{h}(\mathbf{x}(\tau_0), t_0, \mathbf{x}(\tau_f), t_f) = \mathbf{0} \\ \text{The inequality path constraints:} \\ \mathbf{C}(\mathbf{x}(\tau), \mathbf{u}(\tau), \tau; t_0, t_f) \leq \mathbf{0}. \end{array} \right. \quad (2)$$

In the GPM, this optimal control problem is discretized at some specific discretization points, called the Legendre-Gauss (LG) points, and then transcribed into a nonlinear program (NLP) by approximating the states and controls using Lagrange interpolating polynomials [8]. The set of N discretization points includes $K = N - 2$ interior LG collocation points, defined as the roots of the K th-degree Legendre polynomial, the initial point, $\tau_0 = -1$, and the final point, $\tau_f = 1$. An approximation to the state, $\mathbf{X}(\tau)$, is formed with a basis of $K + 1$ Lagrange interpolating polynomials. The control is approximated using a basis of K Lagrange interpolating polynomials; namely $\mathbf{U}(\tau)$. The continuous dynamics are then transcribed into a set of K algebraic constraints via orthogonal collocation. In addition, the integral term in the cost functional can be approximated with a Gauss quadrature.

The resulted NLP are finally found as:

Minimize:

$$J_{\mathbf{x}(\tau_k), \mathbf{u}(\tau_k)} = \Phi(\mathbf{X}(\tau_0), t_0, \mathbf{X}(\tau_f), t_f) + \frac{t_f - t_0}{2} \sum_{i=1}^K \omega_i g(\mathbf{X}(\tau_i), \mathbf{U}(\tau_i), \tau_i),$$

s.t.:

$$\left\{ \begin{array}{l} \mathbf{X}(\tau_f) - \mathbf{X}(\tau_0) - \frac{t_f - t_0}{2} \sum_{i=1}^K \omega_i \mathbf{f}(\mathbf{X}(\tau_i), \mathbf{U}(\tau_i), \tau_i; t_0, t_f) = \mathbf{0} \\ \sum_{i=0}^K \sum_{\ell=0}^K \frac{\prod_{j=0, j \neq i, \ell}^K (\tau_k - \tau_j)}{\prod_{j=0, j \neq i}^K (\tau_i - \tau_j)} \mathbf{X}(\tau_i) - \frac{t_0 - t_f}{2} \mathbf{f}(\mathbf{X}(\tau_k), \mathbf{U}(\tau_k), \tau_k; t_0, t_f) = \mathbf{0} \\ \mathbf{h}(\mathbf{X}(\tau_0), t_0, \mathbf{X}(\tau_f), t_f) = \mathbf{0} \\ \mathbf{C}(\mathbf{X}(\tau_k), \mathbf{U}(\tau_k), \tau_k; t_0, t_f) \leq \mathbf{0}, \quad (k=1, \dots, K) \end{array} \right. \quad (3)$$

In Eq. (3), ω_i are the Gauss weights [10].

The solution of Eq. (3) is an approximate solution to the continuous Bolza problem. In this paper, to solve this NLP, the SNOPT solver is used. SNOPT is a software package for solving large-scale optimization problems. It has been designed for problems with many thousands of constraints and variables, however, it is best suited for problems with a moderate number of degrees of freedom (up to 2000) [12]. It helps us to solve the resulted non-convex optimization problem.

SNOPT uses a Sequential Quadratic Programming (SQP) algorithm. SNOPT makes use of a nonlinear function and gradient values. If some of the gradients are unknown, they will be estimated by finite differences. SNOPT allows the nonlinear constraints to be violated (if necessary) and minimizes the sum of such violations. The main steps of the SNOPT algorithm can be found in [12]. In this paper, we used the SNOPT solver embedded in PROPT software without having to worry about the mathematics of the solver. Once the problem has been properly defined, PROPT takes care of all the necessary steps in order to return a solution.

In order to obtain a solution for the optimal control problem of Eq. (3) as efficiently as possible, while obtaining an accurate solution, 90 Legendre-Gauss collocation points are chosen. While it is beyond the scope of this paper to provide a detailed explanation of various pseudospectral methods and their accuracy, more detailed information can be found in [9,10,13,14].

3. Description of container ship model

A mathematical model for a single-screw, high-speed container ship (often referred to as S175 in the marine engineering community) in surge, sway, roll and yaw, has been presented in [15]. This 4-DoF dynamical ship model is highly nonlinear with 10 states: $\mathbf{x} = [u, v, r, x, y, \psi, p, \phi, n, \delta]^T$ and 2 control inputs: $\mathbf{u} = [n_c, \delta_c]^T$. u, v, r and p are the surge velocity, sway velocity, yaw rate and roll rate, with respect to the ship-fixed frame, respectively. The corresponding displacements, with respect to the inertial frame, are denoted by x, y . ψ and ϕ are the yaw and roll Euler angles. The other two states are the propeller shaft speed, n , and the rudder angle, δ . The inputs to the model are the commanded propeller speed, n_c , and commanded rudder angle, δ_c , respectively. The actuator input saturation and rate limits are also incorporated in this model, so that $|\delta| \leq 35$ deg and $|\dot{\delta}| \leq 5$ deg/s and $0 < n \leq 160$ rpm. The 4-DoF nonlinear model of the vessel is one of the most comprehensive ship models available in open literature. It captures the fundamental characteristics of ship dynamics and covers a wide range of operating conditions. The

nonlinearequations of motion in 4-DoF are given by:

$$\begin{aligned}
 (m' + m'_x)\dot{u}' - (m' + m'_y)v'r' &= X', \\
 (m' + m'_y)\dot{v}' + (m' + m'_x)u'r' + m'_y\alpha'_y\dot{r}' - m'_yl'_y\dot{p}' &= Y', \\
 (I'_x + J'_x)\dot{p}' - m'_yl'_y\dot{v}' - m'_xl'_x u'r' + W'GM'\phi' &= K', \\
 (I'_z + J'_z)\dot{r}' + m'_y\alpha'_y v' &= N' - Y'x'_G.
 \end{aligned} \tag{4}$$

Here, m' denotes the ship mass, and m'_x and m'_y denote the added mass in the x and y directions, respectively. I'_x and I'_z denote the moment of inertia, and J'_x and J'_z denote the added moment of inertia about the x (roll) and z (yaw) axes, respectively. Furthermore, α'_y denotes the x -coordinate of the center of m'_y . l'_x and l'_y are the z -coordinates of the centers of m'_x and m'_y , respectively. W' is the ship displacement, GM' is the metacentric height, and x'_G is the location of the center of gravity in the x -axis. All the primes mean the corresponding dimensionless terms (see Appendix E.1.3 in [15] for details).

The hydrodynamic forces, X' and Y' , and moments, K' and N' , are given by:

$$\begin{aligned}
 X' &= X'_{uu}u'^2 + (1 - tt)T'(JJ) + X'_{vr}v'r' + X'_{vv}v'^2 \\
 &\quad + X'_{rr}r'^2 + X'_{\phi\phi}\phi'^2 + c_{RX}F'_N \sin \delta', \\
 Y' &= Y'_v v' + Y'_r r' + Y'_\phi \phi' + Y'_{vvv}v'^3 + Y'_{rrr}r'^3 \\
 &\quad + Y'_{vvv}v'^2 r' + Y'_{vrr}v'r'^2 + Y'_{vv\phi}v'^2 \phi' \\
 &\quad + Y'_{v\phi\phi}v'\phi'^2 + Y'_{rr\phi}r'^2 \phi' + Y'_{r\phi\phi}r'\phi'^2 \\
 &\quad + (1 + a_H)F'_N \cos \delta', \\
 K' &= K'_v v' + K'_r r' + K'_p p' + K'_\phi \phi' + K'_{vvv}v'^3 \\
 &\quad + K'_{rrr}r'^3 + K'_{vvv}v'^2 r' + K'_{vrr}v'r'^2 \\
 &\quad + K'_{vv\phi}v'^2 \phi' + K'_{v\phi\phi}v'\phi'^2 + K'_{rr\phi}r'^2 \phi' \\
 &\quad + K'_{r\phi\phi}r'\phi'^2 - (1 + a_H)z'_R F'_N \cos \delta', \\
 N' &= N'_v v' + N'_r r' + N'_p p' + N'_\phi \phi' + N'_{vvv}v'^3 \\
 &\quad + N'_{rrr}r'^3 + N'_{vvv}v'^2 r' + N'_{vrr}v'r'^2 \\
 &\quad + N'_{vv\phi}v'^2 \phi' + N'_{v\phi\phi}v'\phi'^2 + N'_{vv\phi}v'^2 \phi' \\
 &\quad + N'_{rr\phi}r'^2 \phi' + N'_{r\phi\phi}r'\phi'^2 \\
 &\quad + (x'_R + a_H x'_H)F'_N \cos \delta',
 \end{aligned} \tag{5}$$

where, tt is the thrust deduction factor, c_{Rx} , a_H and $a_H x'_H$ are interactive forces and moment coefficients

between the hull and rudder, and x'_R and z'_R are the location of the rudder center of effort in x and z directions, respectively. All the coefficients in X' , Y' , K' and N' are the corresponding hydrodynamic derivatives, and their values for S175 are given in Appendix E.1.3 in [15].

The rudder force, F'_N , can be resolved as [15]:

$$\begin{aligned}
 F'_N &= -\frac{6.13\Lambda}{\Lambda + 2.25} \frac{A_R}{L^2} (u'^2_R + v'^2_R) \sin \alpha_R, \\
 \alpha_R &= \delta' + \tan^{-1} \left(\frac{v'^2_R}{u'^2_R} \right), \\
 u'_R &= u'_P \varepsilon \sqrt{1 + 8kK_T / (\pi J J^2)}, \\
 v'_R &= \gamma v' + c_{Rr}r' + c_{Rrrr}r'^3 + c_{Rrrv}r'^2 v',
 \end{aligned} \tag{6}$$

where, Λ is the rudder aspect ratio and A_R is rudder area, and L is the ship length. u'_R and v'_R are inflow velocities of the rudder in x and y directions, respectively, and α_R is the relative angle between the rudder and its inflow. δ' is the rudder angle, and u'_P is the advance speed. ε and k are adjustment constants, and K_T is the propeller thrust coefficient. JJ is the open water advanced coefficient, and γ , c_{Rr} , c_{Rrrr} and c_{Rrrv} are the corresponding hydrodynamic derivatives. Furthermore, the propeller force, T' , in Eq. (5) can be expressed as $T' = 2\rho D^4 K_T n'|n'|$, where D is the propeller diameter and ρ is the water density. Also, the dynamics of the rudder and propeller are incorporated by:

$$\dot{\delta} = (\delta_c - \delta)/T_\delta, \quad \dot{n} = (n_c - n)/T_n. \tag{7}$$

T_δ and T_n are time constants.

The motion equations can be transformed into control-oriented dynamics equations as follows:

$$\begin{aligned}
 &[\dot{u}', \dot{v}', \dot{x}', \dot{y}', \dot{\psi}', \dot{p}', \dot{\phi}', \dot{\delta}', \dot{n}']^T \\
 &= \begin{bmatrix} \frac{X'}{m'_{11}} U^2 / L \\ \frac{-(-m'_{33}m'_{44}Y' + m'_{32}m'_{44}K' + m'_{42}m'_{33}N')}{\det M'} \frac{U^2}{L} \\ \frac{-m'_{42}m'_{33}Y' + m'_{32}m'_{44}K' + m'_{22}m'_{33}N' - m'_{22}N'}{\det M'} \frac{U^2}{L} \\ (u' \cos \psi' - v' \sin \psi' \cos \phi')U \\ (u' \sin \psi' - v' \cos \psi' \cos \phi')U \\ (r' \cos \phi') \frac{U}{L} \\ \frac{-m'_{32}m'_{44}Y' + m'_{22}m'_{44}K' + m'_{42}K' + m'_{32}m'_{44}N'}{\det M'} \frac{U^2}{L} \\ p'U/L \\ (\delta_c - \delta)/T_\delta \\ (n_c - n)/T_n \end{bmatrix}, \tag{8}
 \end{aligned}$$

where, $U = \sqrt{u^2 + v^2}$, $m'_{11} = m' + m'_x$, $m'_{22} = m' + m'_y$, $m'_{32} = -m'_y l'_y$, $m'_{42} = -m'_y \alpha'_y$, $m'_{33} = I'_x + J'_x$, $m'_{44} = I'_z + J'_z$ and $\det M' = m'_{22} m'_{33} m'_{44} - m'^2_{32} m'_{44} - m'^2_{42} m'_{32}$.

4. Simulations and results

4.1. Nonlinear optimal tracking

Economy (minimum fuel usage), safety (related to accuracy and maneuverability), and user preferences are three major factors that should be considered in path tracking [16].

These demands should be translated into a performance criterion function to be minimized by an optimal control system. Since the ship control configuration is required to minimize the heading error for a desired heading, ψ_d , minimize the propeller shaft speed, n_c , for minimum fuel cost, and minimize the rudder deflection angle δ_c , the cost function to be minimized is chosen as:

$$J = \int_0^{t_f} (P(\psi - \psi_d)^2 + Qn_c^2 + R\delta_c^2) dt. \quad (9)$$

The above cost function balances accurate tracking against reduced actuator usage, because they are both dependent on each other. P , Q and R are the corresponding weighting coefficients. The more the value of P , the more accurate tracking is achieved. On the other hand, if the value of Q in the cost function is increased, the shaft speed and fuel consumption will be decreased. By increasing the value of R , the rudder deflection will be decreased. Note that the vessel roll angle, rudder angle and its rate limits are considered as inequality constraints ensured us from their satisfaction.

4.1.1. Effects of weighting matrices P , Q and R

The weighting matrices, P , Q and R , are used as the main tuning parameters to shape the closed-loop response for the desired performance [17]. Assume that the vessel initial state is zero and the desired heading, ψ_d , should be reached at 95 degrees.

Figure 1 depicts the states of container ship dynamics, together with actuator dynamics of the vessel, for $P = 10^2$, $Q = 0$ and $R = 0$. The heading angle of the vessel reaches the desired value. The container starts the mission with maximum propeller shaft speed. There is no limit of fuel usage in the cost functional in this scenario, so, maximum shaft speed is expected. The values of roll and rudder angle do not exceed their limits.

Another simulation with different gains of $P = 10^2$, $Q = 10^3$ and $R = 10^3$ is performed and its results are shown in Figures 2. As seen in Figure 2, increasing the value of the propeller shaft speed gain in the cost functional of Eq. (9) results in a reduction in fuel cost.

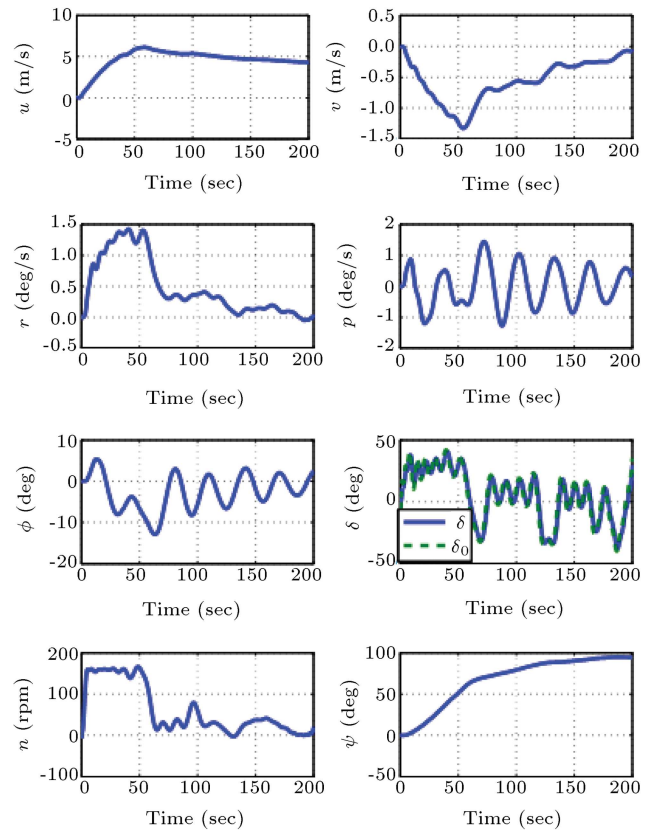


Figure 1. The states of container ship dynamics for $P = 10^2$, $Q = 0$ and $R = 0$.

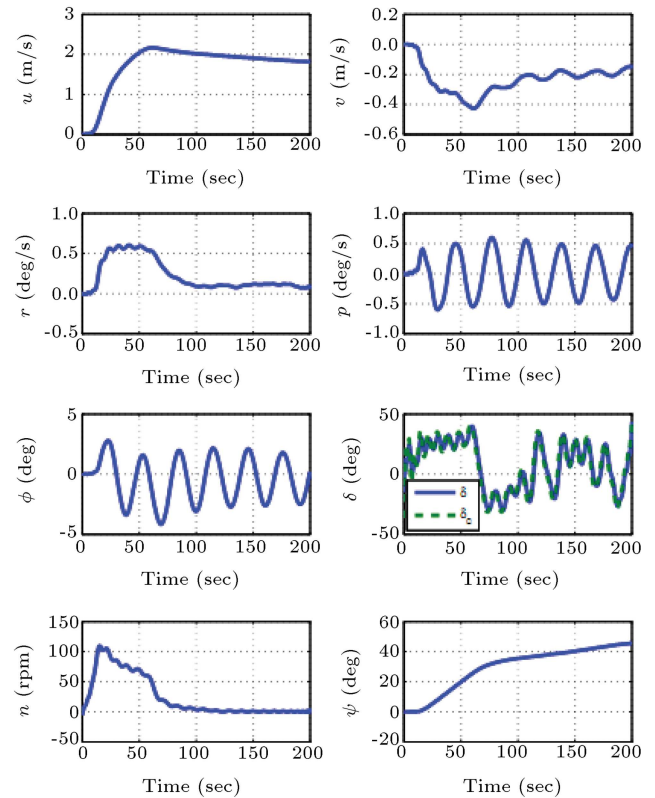


Figure 2. The states of container ship dynamics for $P = 10^2$, $Q = 10^3$ and $R = 10^3$.

The heading angle does not reach the desired value of 95 degrees, because its gain in the cost function is much less than the gain of the propeller shaft speed.

The results of two simulations indicate that, if the controller minimizes heading error too much, this, in turn, would require an extreme control effort, resulting in unnecessary extra costs, such as fuel consumption. On the other hand, if the actuator usage is kept to a minimum, the heading error will be too large, since the control effort would be insufficient to keep the desired response.

These simulations were run on a laptop with a Windows 7 Operating System (OS), an Intel Core i5 2.27 GHz processor, and 4 GB of Random Access Memory (RAM). The mean computation time for a 90-node solution is approximately 45 seconds, meaning that the computational time is low.

4.1.2. Enforcing roll constraints

Generally, a trade-off exists between the tracking performance and the roll minimization, namely, imposing roll constraints will deteriorate the tracking performance of vessels. To understand this trade-off, assuming that the initial state of the vessel is chosen to be $\mathbf{x}_0 = [6\frac{m}{s}, 0, 0, 0, 0, 0, 0, 0, 66 \text{ rpm}, 0]^T$ and the propeller shaft speed is to be constant at 90 rpm, simulations are performed with different roll constraints imposed, and the results are summarized in Figure 3. From Figure 3, we can see that, the more the roll constraint is tightened, the less tracking performance is achieved. This is because the large rudder action is not permissible due to the roll constraints. When there is no roll constraint, the vessel reaches the desired heading, but, for roll constraint of 7 deg, the desired heading is not achieved. For roll constraint of 3 deg, the heading error is high, needing more time to converge

to zero. However, since the roll angle of the vessels seriously increase in the presence of wave loads [18], enforcing roll constraints while maneuvering in seaways should be considered.

4.2. Course-changing autopilot

During course-changing maneuvers (path tracking), it is desirable to specify the dynamics of the desired heading instead of using a constant reference signal presented in the course-keeping mode. The amount of change in the heading angle is determined from the desired heading the controller needs to track, which is commanded either by a helmsman/pilot or an autopilot [19].

In the simulations performed in this section, the desired heading response has been commanded by $\psi_c = 0.0025 * \pi t$, which makes the ship track a circular path [20]. The initial state of the vessel is chosen to be $\mathbf{x}_0 = [6\frac{m}{s}, 0, 0, 0, 0, 0, 0, 0, 66 \text{ rpm}, 0]^T$ and it is assumed that the propeller shaft speed is to be constant at 66 rpm. The roll angle limit is $|\phi| \leq 20$ deg.

To track the mentioned pilot input, a quadratic cost functional is defined as follows:

$$J = \int_0^{t_f} (P(\psi - \psi_c)^2 + R\delta_c^2) dt. \tag{10}$$

Figure 4 shows the vessel course in the earth-fixed coordinate for $P = 10^3$ and $R = 10$. The vessel starts to move from the origin and track the reference heading.

Figure 5 depicts the states of the ship dynamic model. The motion of the rudder produces drag forces that slow down the vessel during turning. The values of roll and rudder angles do not exceed their limits. The rudder system of the vessel is a first order system with a one second delay time (Eq. (7)). So there is a little

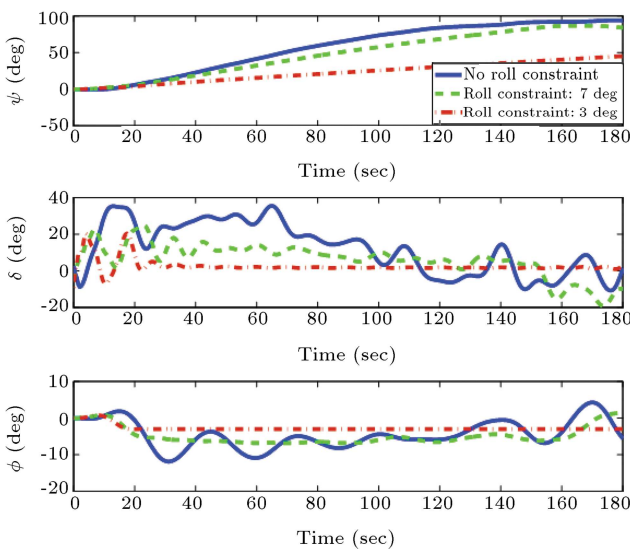


Figure 3. Simulation results of the ship response with different roll constraints.

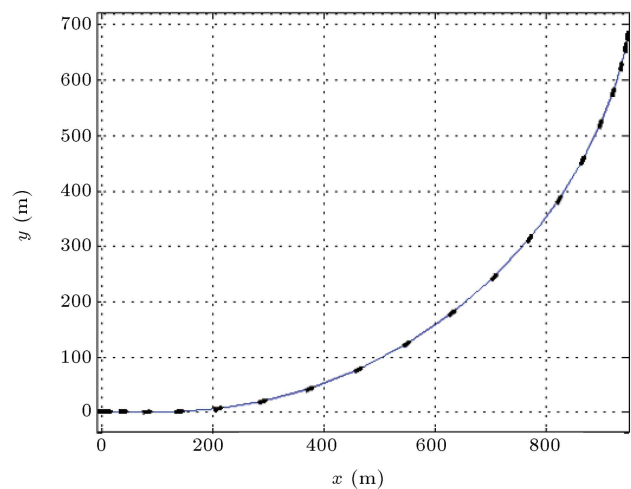


Figure 4. The vessel course in the earth-fixed coordinate for course changing maneuver.

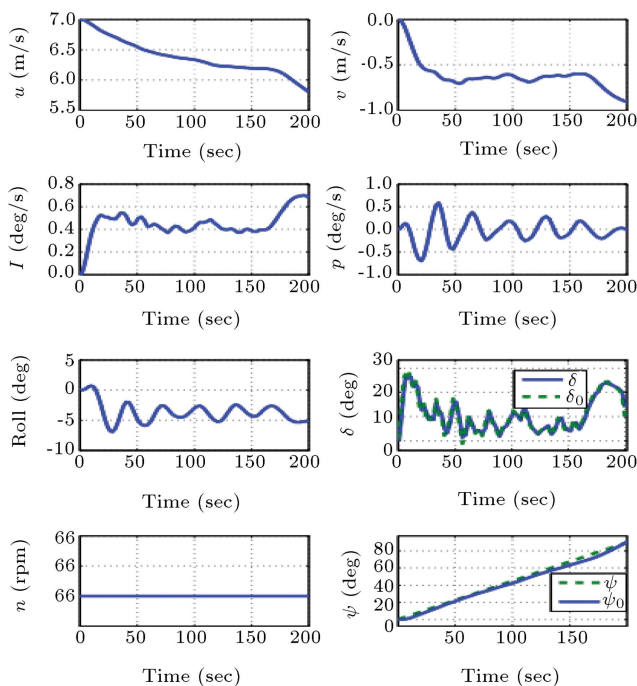


Figure 5. The states of ship dynamic model for course changing maneuver.

difference between the commanded and actual rudder angles. As seen in Figure 4, the vessel exactly tracks the commanded heading of the helmsman or autopilot system.

5. Conclusion

In this paper, an optimal control approach, addressing the tracking control of underactuated marine surface vessels, is presented. The detailed optimal controller formulation and its transcription to NLP via direct GPM is described. The simulation results for course-keeping and course-changing maneuvers show that GPM can achieve precise tracking control of marine surface vessels, while satisfying the prescribed input and state constraints, without needing to linearize their dynamical models.

References

- Do, K.D. and Pan, J., *Control of Ships and Underwater Vehicles: Design for Underactuated and Nonlinear Marine Systems*, Springer (2009).
- Lefeber, E., Pettersen, K.Y. and Nijmeijer, H. "Tracking control of an underactuated ship", *IEEE Transactions on Control Systems Technology*, **11**, pp. 52-61 (2003).
- Jiang, Z.P. "Global tracking control of underactuated ships by Lyapunov's direct method", *Automatica*, **38**, pp. 301-309 (2002).
- Avgouleas, K. "Optimal ship routing", MSc Thesis, Department of Mechanical Engineering, Massachusetts Institute of Technology, United States, Massachusetts (2008).
- Li, Z., Sun, J. and Oh, S. "Path following for marine surface vessels with rudder and roll constraints: An MPC approach", in *American Control Conference*, St. Louis, MO, USA, pp. 3611-3616 (2009).
- Ghaemi, R. "Robust model based control of constrained systems", Ph.D. Thesis, The University of Michigan (2010).
- Çimen, T. and Banks, S.P. "Nonlinear optimal tracking control with application to super-tankers for autopilot design", *Automatica*, **40**, pp. 1845-1863 (2004).
- Betts, J.T. "Survey of numerical methods for trajectory optimization", *Journal of Guidance, Control, and Dynamics*, **21**, pp. 193-207 (1998).
- Benson, D. "A Gauss pseudospectral transcription for optimal control", Ph.D. Thesis, Massachusetts Institute of Technology, United States, Massachusetts (2005).
- Huntington, G. "Advancement and analysis of a Gauss pseudospectral transcription for optimal control problems", Ph.D. Thesis, Massachusetts Institute of Technology, United States, Massachusetts (2007).
- Trefethen, L.N., *Spectral Methods in Matlab*: Society for Industrial and Applied Mathematics (2000).
- Gill, P.E., Murray, W. and Saunders, M.A. "SNOPT: An SQP algorithm for large-scale constrained optimization", *SIAM Review*, **47**, pp. 99-131 (2005).
- Garg, D., Patterson, M., Hager, W.W., Rao, A.V., Benson, D.A. and Huntington, G.T. "A unified framework for the numerical solution of optimal control problems using pseudospectral methods", *Automatica*, **46**, pp. 1843-1851 (2010).
- Salarieh, H. and Ghorbani, M. "Trajectory optimization for a high speed planing boat based on gauss pseudospectral method", *The 2nd International Conference on Control, Instrumentation and Automation (ICCIA 2011)*, Shiraz University (2011).
- Fossen, T.I., *Guidance and Control of Ocean Vehicles*, Wiley (1994).
- Çimen, T. "On-line nonlinear optimal maneuvering control of large tankers in restricted waterways", *The 7th IFAC Conference on Manoeuvring and Control of Marine Craft (MCMC'2006)*, Lisbon, Portugal (2006).
- Kirk, D.E., *Optimal Control Theory: An Introduction*, Dover Publications (2004).
- Banazadeh, A. and Ghorbani, M.T. "Frequency domain identification of the Nomoto model to facilitate Kalman filter estimation and PID heading control of a patrol vessel", *Ocean Engineering*, **72**, pp. 344-355 (2013).
- Çimen, T. "Development and validation of a mathematical model for control of constrained non-linear

oil tanker motion”, *Mathematical and Computer Modelling of Dynamical Systems*, **15**, pp. 17-49 (2009).

20. Cheng, J., Yi, J. and Zhao, D. “Design of a sliding mode controller for trajectory tracking problem of marine vessels”, *IET Control Theory & Applications*, **1**, pp. 233-237 (2007).

Biographies

Mohammadtaghi Ghorbani was born in Kashan, Iran, in 1987. He received his BS degree in Mechanical Engineering from Kashan University, Kashan, Iran, in

2009, and his MS degree in Mechatronic Engineering in 2012 from Sharif University of Technology, Tehran, Iran. His special fields of interest include optimization and optimal control.

Hassan Salarieh received his BS degree in Mechanical Engineering and Pure Mathematics, in 2002, and MS and PhD degrees in Mechanical Engineering in 2004 and 2008, respectively, from Sharif University of Technology, Tehran, Iran, where he is currently Associate Professor in Mechanical Engineering. His fields of research are dynamical systems, control theory and stochastic systems.